Journal of Chromatography, 387 (1987) 65–84
Elsevier Science Publishers B.V., Amsterdam — Printed in The Netherlands

CHROM. 19 103

DETERMINATION OF PORE SIZE DISTRIBUTION CURVES BY SIZE-EXCLUSION CHROMATOGRAPHY

JOHN H. KNOX* and HARALD J. RITCHIE
Department of Chemistry, University of Edinburgh, West Mains Road, Edinburgh EH9 3JJ (U.K.)
(First received July 7th, 1986; revised manuscript received September 9th, 1986)

SUMMARY

The mathematical formulation of the relationship between the pore size distribution (PSD) and the size-exclusion chromatography calibration (SECC) curve for a rigid porous material originally developed by Knox and Scott has been extended and computerized.

Knox and Scott [*J. Chromatogr.*, 316 (1984) 311–332] showed that the SECC could be accurately predicted from the PSD obtained by mercury porosimetry on the assumption that the pores of the material were cylindrical and that the probe molecules (polystyrenes) could be regarded as spheres, and that the reverse procedure was also possible by a simple mathematical procedure. We have found that their original procedure cannot unfortunately be computerized because of the difficulty of fitting a smooth mathematical function to the experimental SECC, and we have examined several alternative methods. Of these the most successful selects an optimum single pore size and then builds around this a distribution of pores whose sizes fall in geometrical progression. The program can be implemented by a microcomputer using up to seven pore contributions, or in a more powerful procedure by a mainframe computer which can also allow for incomplete penetration of the smallest sample probe and incomplete exclusion of the largest sample probe.

We recommend adoption of our procedure in place of the widely used method of Halasz and Martin [*Ber. Bunsenges. Phys. Chem.*, 79 (1975) 731–4; *Angew. Chem., Int. Ed. Engl.*, 17 (1978) 901–908].

INTRODUCTION AND THEORY

Porous solids are of prime importance in chromatography, as catalysts, as catalyst supports and as adsorbents generally. In relating their performance to their physical and chemical properties, it is important to understand as much as possible about their internal structure including their surface area, mean pore size and pore size distribution (PSD).

This paper is devoted to determining PSDs of rigid porous materials which are suitable for modern high-performance liquid chromatography (HPLC) using data from size-exclusion chromatography calibration (SECC) curves. Typical of such ma-

0021-9673/87/$03.50

terials are silica gels, rigid macroporous polystyrenes, porous glasses, and other materials containing mainly meso- and macropores. In these materials there is a clear distinction between the solid structure and the pore space so that the internal surface area and the pore volume are both well defined. In general pores may be grouped into three classes[1]: (a) micropores, having radii below 10 Å; (b) mesopores, having radii between 10 and 500 Å; (c) macropores, having radii larger than 500 Å.

PSDs in the mesopore range and above can be found by three main methods: (a) gas adsorption–desorption isotherms at high relative pressures of adsorbate; (b) mercury porosimetry; (c) size exclusion chromatography (SEC).

The determination of PSDs by gas adsorption relies on interpretation of the adsorption isotherm of a gas such as nitrogen. Materials which contain mesopores give type IV isotherms according to the Brunnauer–Emmett–Teller classification[2] and exhibit a hysteresis loop at relative vapour pressures of adsorbate, p/p_0, between 0.4 and 1.0. The method depends upon the fact that the vapour pressure, p, of a liquid above a curved concave of radius, R, is less than the vapour pressure, p_0, above a flat surface, being given by the Kelvin equation:

$$\ln(p/p_0) = -2V_m\gamma \cos\theta/(RRT) \tag{1}$$

where θ is the contact angle, γ the surface tension of liquid adsorbate, V_m the molar volume of liquid adsorbate, R the universal gas constant and T the absolute temperature. When R falls within the mesopore range, 10–500 Å, capillary condensation occurs within such pores at pressures which are significantly below p_0. Accordingly the volume of pores up to a particular radius, R, can be found from the volume of liquid adsorbate taken up by the material when the pressure is increased up to the pressure, p, given by eqn. 1. Generally type IV adsorption isotherms show a hysteresis loop; that is, the plot of amount adsorbed against relative pressure p/p_0 follows a lower curve during adsorption than during desorption. There is considerable argument about the interpretation of the hysteresis loop and this is discussed in detail by Gregg and Sing[3]. The most plausible explanation when dealing with materials made up of coalesced spherical colloidal units seems to be that initial capillary condensation occurs around the cusp-shaped regions where the colloidal spheres touch. This condensation is reversible and so does not enter into the hysteresis loop. At higher relative pressures condensation occurs in the narrow channels formed by trios of spheres. These channels lead into larger cavities. It is likely that at a certain stage these cavities become isolated by condensation in all the channels which lead into them[4]. Subsequently these cavities are filled at relative pressures which are appropriate to their radii. However, on reducing the relative pressure to determine the desorption branch of the isotherm, any particular cavity will not empty until the widest channel leading into it has emptied. Cavity filling and emptying are not therefore reversible so a well defined hysteresis loop is produced which does not depend upon the time allowed for equilibration. If this explanation is correct then the pore size distribution should be determined from the adsorption branch of the isotherm not from the desorption branch.

The method of determining the PSD using eqn. 1 makes several assumptions. It assumes, first that the pores are cylindrical; secondly that the contact angle is known; and thirdly that the surface tension of the liquid adsorbate is constant down

to very small radii of curvature of the liquid surface. All three assumptions are suspect. In addition, by the stage that capillary condensation occurs, the internal surface of the adsorbent will already be covered by at least a monolayer of adsorbate which will reduce the radii of all pores by the monolayer thickness leading to low values of the pore size unless a correction is made.

The determination of the PSD by mercury porosimetry is based upon eqn. 2 due to Washburn which gives the excess pressure required to maintain a convex spherical surface of radius, R

$$\Delta p = 2\gamma \cos \theta / R \tag{2}$$

Mercury is commonly used as the non-wetting liquid, and with pressures up to 5000 bar it is possible to penetrate pores with radii as small as 10 Å. The method again assumes that the pores are cylindrical, that the contact angle is known and that the surface tension of mercury is independent of the radius of its surface. Since the mercury porosimetry method depends upon penetration of cavities through their entrance channels, the penetration of any cavity will occur at a pressure determined by the radius of the widest entry channel rather than the radius of the cavity itself. On reduction of pressure these cavities may not all empty, leading to the so-called "ink-bottle" effect. Mercury porosimetry will give PSDs which are directly comparable to those obtained from the desorption branch of the adsorption isotherm, and should give slightly smaller pore radii than those determined from the adsorption branch of the isotherm.

Methods based upon SEC use molecules of known or assumed radius to probe the pores of the material. Random coil polymers such as polystyrenes are commonly used. As Casassa[5] has shown such molecules can be regarded for this purpose as behaving as if they were rigid spheres. Nevertheless because of their real flexibility they are able to pass through channels whose radii are actually smaller than the effective sphere-radius of the polymer molecule itself, and can therefore explore the entire pore structure of a material even when it contains ink-bottle pores.

In practice one measures the retention volume, V_R, of a range of polymers of different molecular weights, the polymer samples having low polydispersities. Care is taken to avoid adsorption by using a good solvent as eluent. The retention volume will then lie between the extra-particle void volume, V_0, and the total volume of eluent within the column, V_m. The degree of permeation into the pores of the material (pore volume, $V_p = V_m - V_0$) is characterised by the permeation coefficient, K, defined by eqn. 3:

$$K = (V_R - V_0)/(V_m - V_0) \tag{3}$$

V_m is normally found using a small molecule as probe, for example benzene, while V_0 is found using a molecule of sufficiently high molecular weight that it will be excluded from all the pores of the material. Both of these assignments are somewhat arbitrary and, as we point out later, this has to be allowed for in fitting theoretical to experimental values of K.

Most recent work on the determination of PSD curves from SECC curves[6–10] uses the method of Halasz and Martin[11,12] which assumes that for a uniform array

of cylindrical pores of radius R, any molecule of radius greater than R will have $K = 0$, while any molecule of radius less than R will have $K = 1$. As pointed out by Knox and Scott[13] the second of these assumptions is incorrect, and it forced Halasz and Martin to assume that in SEC polystyrene molecules had an apparent radius 2.5 times greater than that given in well established formulae[14,15] of which we use that of Van Krefeld and Van den Hoed[15]

$$r/\text{Å} = 0.123M^{0.588} \tag{4}$$

(where M is the relative molecular weight of the polystyrene molecule). The correct formulation for the permeation coefficient of a spherical molecule of radius, r, into cylindrical pores is given by eqns. 5, 6 and 8.

For an array of uniform cylinders of radius R,

$$K(r) = \left(1 - \frac{r}{R}\right)^2; \; r < R: \; K = 0; \; r > R \tag{5}$$

For an assembly of cylinders with a continuous distribution of radii, such that a fraction $G'(R)\mathrm{d}R$ of the pore volume is taken up by cylinders of radii between R and $R + \mathrm{d}R$

$$K(r) = \int_r^\infty G'(R)\left(1 - \frac{r}{R}\right)^2 \mathrm{d}R \tag{6}$$

The differential pore size distribution function, $G'(R)$, is related to the cumulative pore size distribution function, $G(R)$, by eqn. 7:

$$G(R) = \int_0^R G'(R)\mathrm{d}R \tag{7}$$

For an assembly of cylindrical pores with discrete radii where a fraction $F(R)$ of the total pore volume is taken up in pores of radii R,

$$K(r) = \sum_{R=r}^{R=\infty} F(R)\left(1 - \frac{r}{R}\right)^2 \tag{8}$$

Knox and Scott[13] showed that for a continuous distribution of pore diameters, $G(R)$ could be obtained from the plot of $K(r)$ again ln r by a simple differentiation procedure as given in eqn. 9

$$G(R) = K(r) - \frac{3}{2}\left[\frac{\mathrm{d}\,K(r)}{\mathrm{d}\ln r}\right] + \frac{1}{2}\left[\frac{\mathrm{d}^2K(r)}{\mathrm{d}(\ln r)^2}\right] \tag{9}$$

They used a graphical method to differentiate the plot of $K(r)$ against ln r. Unfor-

tunately this method was time consuming, subjective and showed instability. In this paper, *inter alia*, we have sought a procedure whereby an analytical expression could be computer fitted to the [$K(r)$, ln r] curve and from which the [$G(R)$, ln R] curve could be derived by eqn. 9.

Unlike the previous methods, the SECC method for determining the PSD of a material requires no assumptions about contact angle or surface tension at low radii of curvature, but it does assume that the polymer probe has zero enthalpy of transfer from the bulk solvent outside the particles to the solvent within the pores of the SEC material. Accordingly, the SEC method should provide PSDs with fewer assumptions than the adsorption and mercury porosimetry methods. PSDs derived from SEC curves should be comparable to those obtained from the adsorption branch of the hysteresis loop of the adsorption isotherm and may indicate slightly larger pores than those given by mercury porosimetry, since the latter sees ink-bottle pores as having the radii of their entrance channels.

We would argue that PSDs derived from SECC curves are likely to be the most relevant if the PSD information is actually required for a chromatographic application.

PROCEDURES AND GENERAL CONSIDERATIONS

In devising any procedure for matching SECC and PSD curves one has to recognise two problems in fitting theoretical and experimental $K(r)$ values. First of all, the small molecule which is assigned an experimental $K(r)$ value of unity will, having a finite radius, be slightly excluded from the pore space and will therefore have a theoretical $K(r)$ value just below unity. Secondly, the largest probe molecule, which is assigned an experimental $K(r)$ value of zero may have a non-zero theoretical $K(r)$ value. This can arise as follows. As shown by Fig. 1, there is no clear distinction

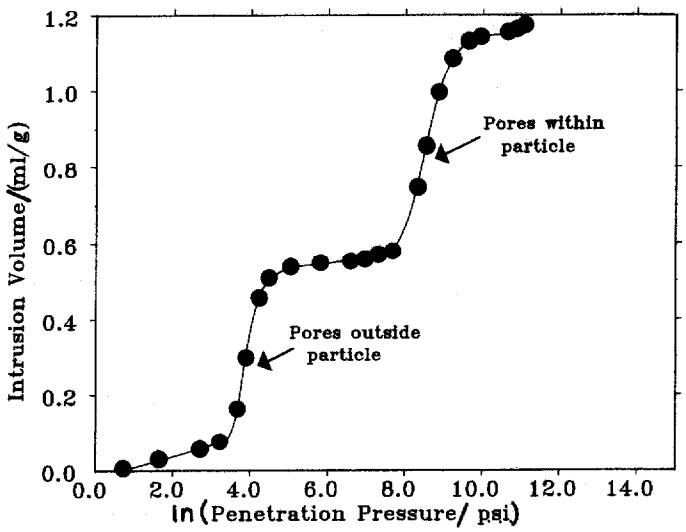

Fig. 1. High-pressure mercury porosimetry data for a typical 5-μm silica gel PR-179 having a narrow pore size distribution.

between the intra-particle pore volume and the inter-particle void space. There can thus be no sense in which a large probe molecule can be said to be totally excluded from a clearly defined set of intra-particle pores. Thus any calculated value of $K(r)$ for a large molecule of a size comparable with the largest intra-particle pores using a trial PSD will most likely be non-zero. We allow for these possibilities by defining an adjusted $K(r)$ value which is related to the experimental $K(r)$ value by eqn. 10:

$$K(r)_{adj} = \alpha + \beta K(r)_{exp} \tag{10}$$

α is now the adjusted $K(r)$ value for the "excluded" solute, and $(\alpha + \beta)$ the adjusted $K(r)$ value for the "fully permeating" solute. The constants α and β may be arbitrarily chosen or may be optimised along with the PSD curve to achieve the best fit between theoretical and experimental $K(r)$ data.

We have examined three procedures for deriving PSDs from SECC curves. In each case we optimise the values of a number of parameters to obtain the best fit between calculated and experimental $K(r)$ values. The control function, which is minimised, is the variance, V, between calculated and experimental $K(r)$ values: V is evaluated by

$$V = \sum_{\substack{\text{all} \\ \text{data} \\ \text{points}}} [K(r)_{adj} - K(r)_{th}]^2 \tag{11}$$

In general K_{adj} will be given by eqn. 10 but where it is not convenient to make any adjustment to the experimental values α is taken as zero and β as unity so that K_{exp} is used directly without adjustment.

In the first procedure we attempted to improve the manual method of Knox and Scott[13] by fitting a polynomial to the $[K(r), \ln r]$ data. The coefficients of the polynomial were adjusted to minimise V before applying eqn. 9.

The second procedure assumed a mathematical expression for $G'(R)$ as a function of R (for example a skewed Gaussian) and a theoretical $[K(r), \ln r]$ curve was derived using eqn. 6. The coefficients in the trial function for $G'(R)$ were adjusted to minimise V.

In the third and most general procedure a step-function PSD was assumed comprising a set of discrete pores of radii R_1 to R_N ($N \leqslant 7$). $K(r)$ was then found for each r value using eqn. 7, and the volume fractions F_1 to F_N for each pore size were adjusted to minimise V: optimisation of α and β could also be included.

Method 1. Best fit of a polynomial to [K(r), ln r] Data

Polynomials of degrees from 3 to 8, given by eqn. 12 were fitted to typical exclusion data

$$K_{adj} = a_0 + a_1(\ln r) + a_2(\ln r)^2 + \ldots + a_n(\ln r)^n \tag{12}$$

As the degree of the polynomial was increased, progressively lower values of V were obtained but, as seen from Fig. 2 and 3, the higher degree polynomials gave unacceptable $[K(r), \ln r]$ curves with waves, a well known feature of this method of curve

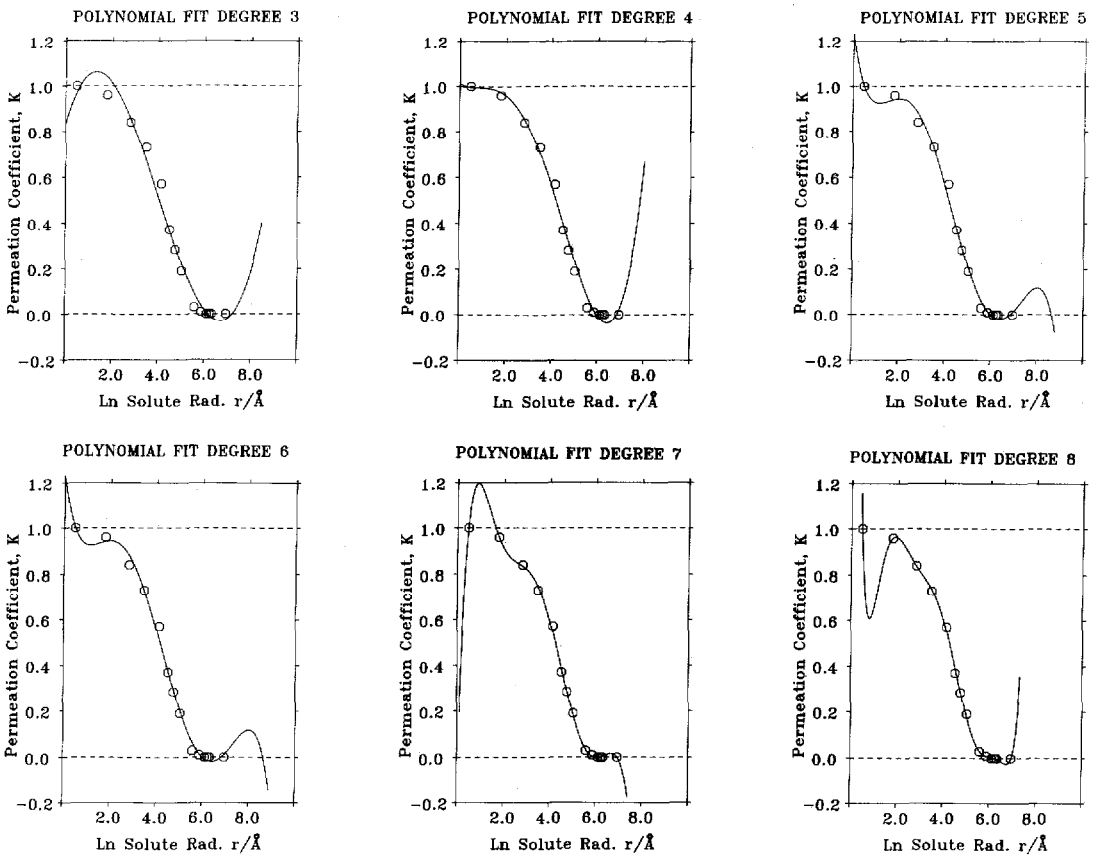

Fig. 2. Best fits of polynomials of degrees 3 to 8 to [$K(r)$, ln r] data for silica gel HR-WPS-2, an experimental wide-pore silica gel (method 1).

fitting. Differentiation according to eqn. 9 accentuated these waves and gave unacceptable PSD curves with both negative $G(R)$ values and values exceeding unity as seen in Figs. 4 and 5. Such effects could be avoided by limiting n but comparing Figs. 4 and 5, it is seen that no unique degree of polynomial gives an adequate fit for these two particular materials.

We conclude, as did Warren and Bidlingmeyer[16], that a polynomial cannot in general be successfully fitted to [$K(r)$, ln r] data, and therefore that the approach, using eqn. 9 to obtain the PSD, is not likely to be successful. Nevertheless, as shown later, a reasonable PSD can be obtained, at least in some cases, if $G(R)$ values outside the limits 0 and 1 are simply ignored. It would, however, be dangerous to assume that this could be applied to all cases.

Method 2. Optimisation of an assumed function for G'(R)

In this procedure a skewed Gaussian distribution was assumed for the differential PSD curve. α and β of eqn. 10 were taken as zero and unity respectively and eqn. 7 used to compute the [$K(r)$, ln r] data. The skewed Gaussian is formed by

adding together a series of Gaussian profiles whose heights decrease exponentially with distance from the centre of the first member of the series. The primary Gaussian curve is given by

$$G'(R) = \frac{1}{\sqrt{2\pi\sigma^2}} \exp[-(\ln R - \ln \mu)^2/2\sigma^2] \tag{13}$$

where μ is the radius of the central pore and σ is the standard deviation of the curve in units of ln R. The formula for the skewed Gaussian is given by eqn. 14 where α is the exponential decay factor.

$$G'(R) = \frac{\alpha}{\sqrt{\pi\sigma^2}} \exp\left[-\frac{2\alpha(\ln R - \ln \mu) - \alpha^2\sigma}{2\sigma}\right] \cdot \operatorname{erfc}\left[\frac{\alpha\sigma - (\ln R - \ln \mu)}{\sqrt{2\sigma^2}}\right] \tag{14}$$

An example of the best fit obtained by optimizing μ, σ and α is shown in Fig. 6. The fit to the SECC data is good at low values of r but a systematic deviation is seen at intermediate values. This is observed even with a material having a very narrow pore

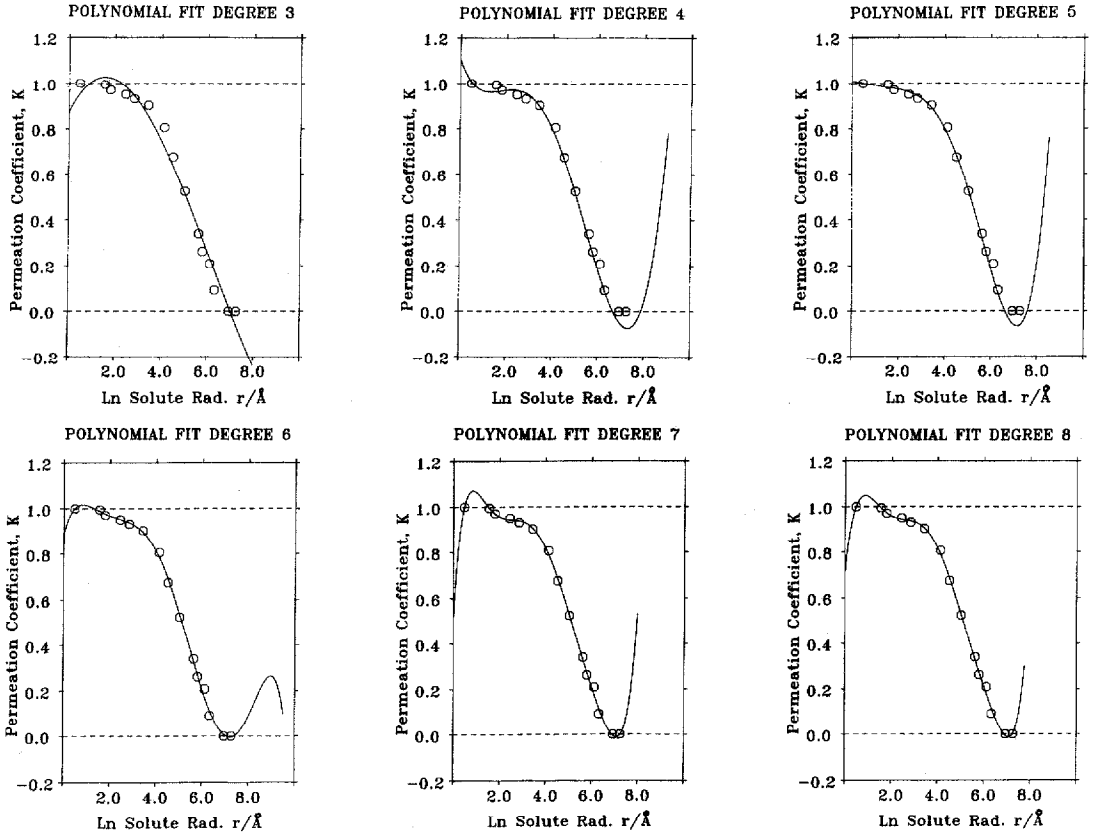

Fig. 3. As for Fig. 2. Data for silica gel PSM 1000 (DuPont material).

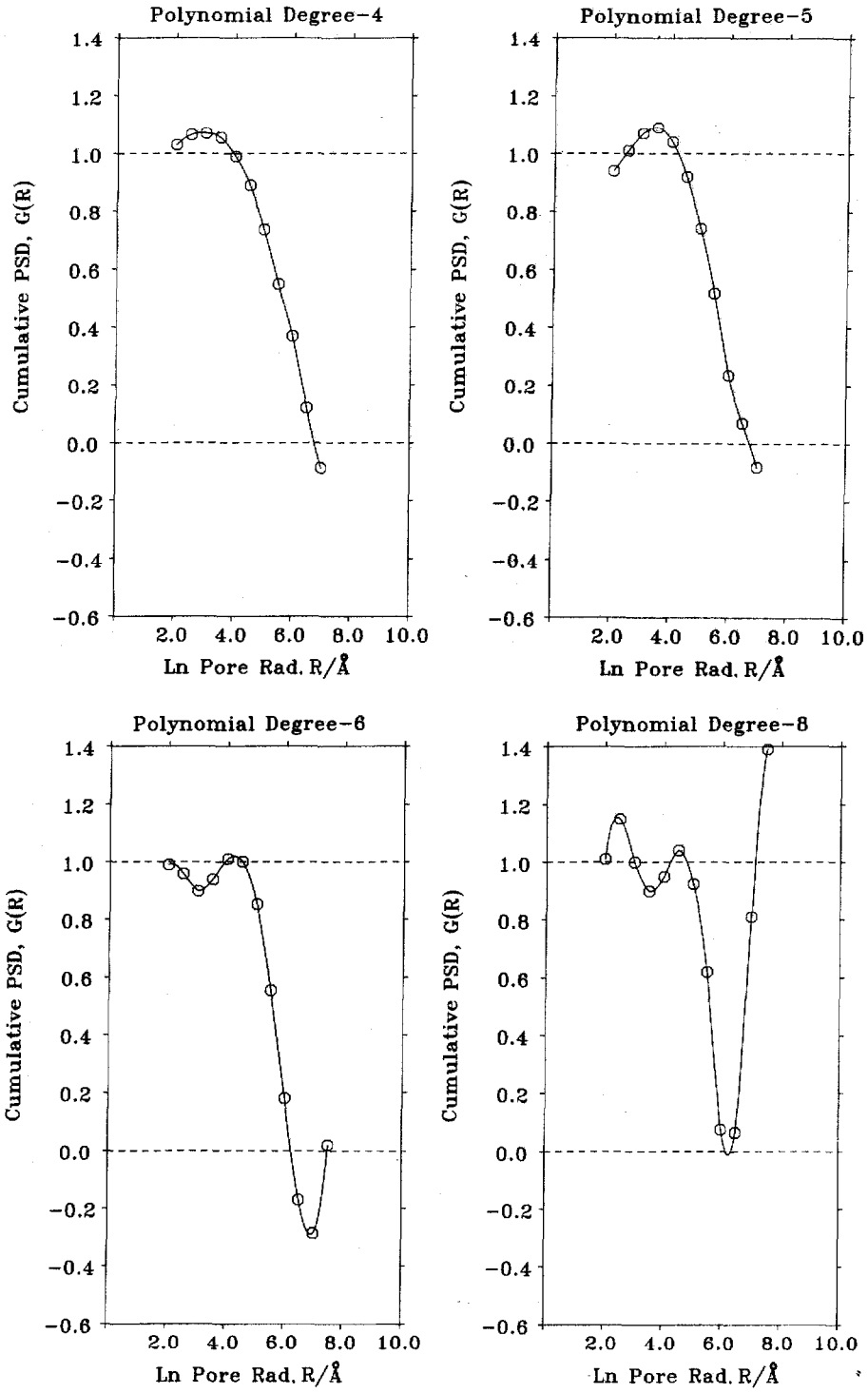

Fig. 4. PSD curves derived from best fit polynomials of degree 4, 5, 6 and 8 to data for silica gel HR-WPS-2 (method 1). Note the excursions of $G(R)$ beyond the limits zero and one.

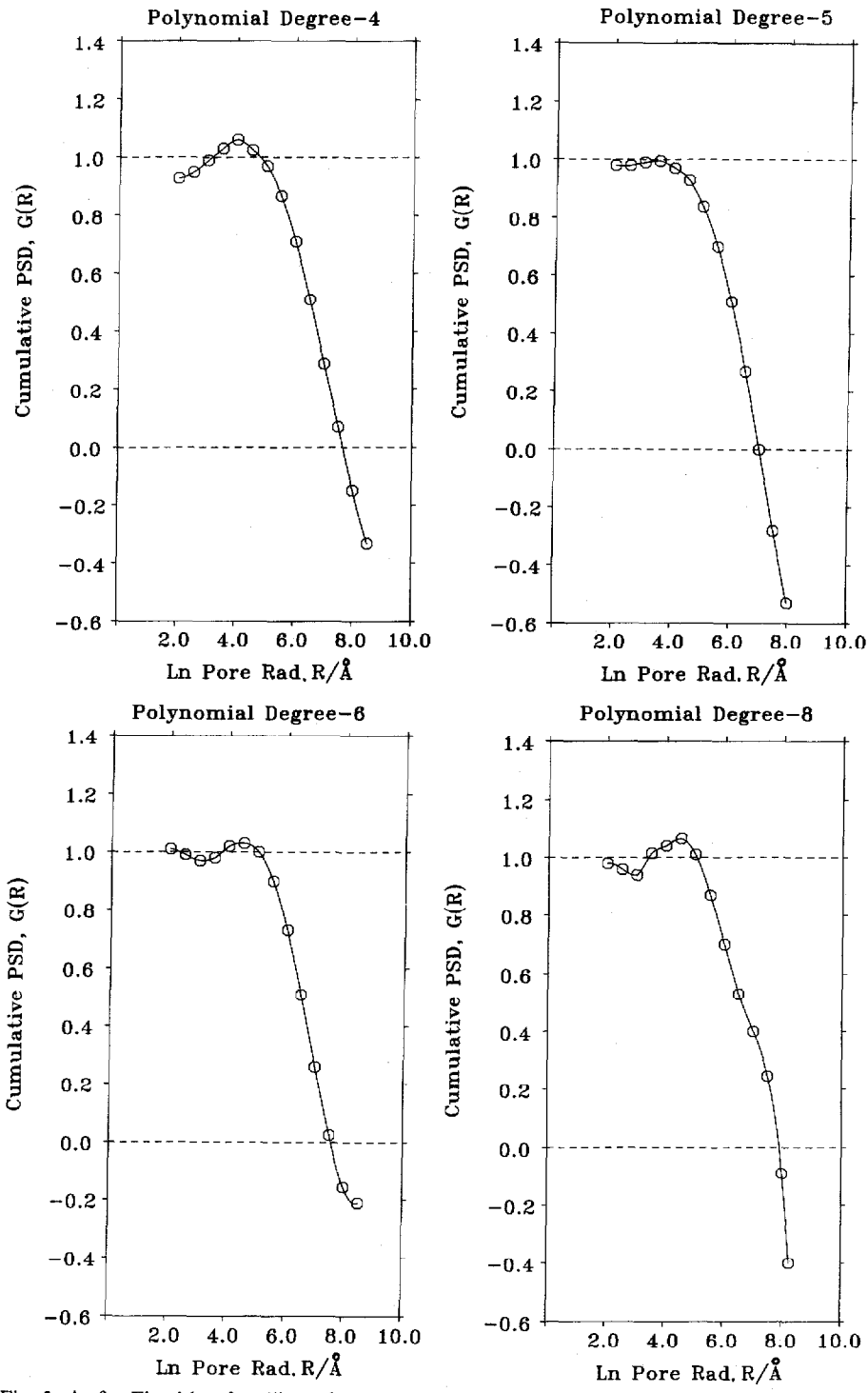

Fig. 5. As for Fig. 4 but for silica gel PSM 1000.

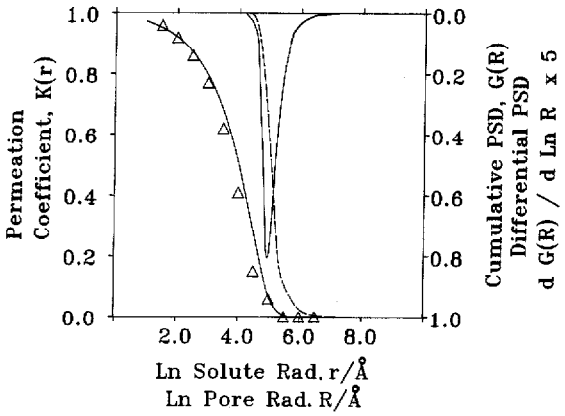

Fig. 6. Best correlation of a skewed Gaussian PSD function with the experimental [$K(r)$, ln r] data obtained for Hypersil (silica gel marketed by Shandon Southern Products) (method 2). Points are experimental data with calculated line superimposed: full line is $G'(R)$ *versus* R curve; broken line is $G(R)$ *versus* R curve.

size range. The fit is likely to be much worse when the method is applied to materials with wide PSDs. Evidently restriction to three adjustable parameters, at least in this form, is too severe. We conclude that an adequate fit could be found only when the chosen expression for $G(R)$ or $G'(R)$ contained at least four adjustable parameters.

Method 3A. Optimisation of the volume fractions of a set of pores of preselected radii using a microcomputer

With a failure of analytical forms adequately to represent either the SEC curve or to predict the SEC curve from an assumed form of PSD curve, methods were examined in which a set of pores of arbitrary radii was selected and the volume-fraction of each pore optimized by microcomputer to provide the best fit to the experimental data using eqns. 8 and 11.

A direct interactive method was first examined in which various trial PSDs were tested following determination of the single pore size R_0 which gave the best fit to the [$K(r)$, ln r] data. Intervention by the operator enabled changes in V to be examined which were brought about by:

(1) altering the PSD for a given selection of pore sizes;

(2) changing the number of pores in the PSD;

(3) changing the spacing of the pore radii in the PSD.

At this stage α and β of eqn. 10 were taken as zero and one respectively.

After some practice the operator was able to determine an optimum PSD relatively quickly by what was essentially a trial and error procedure. It soon became clear that the number of different pore radii which could usefully be optimized was limited to about seven after which addition of further pores of new radii led to little or no improvement in the variance.

A flow diagram for the interactive program is given in Fig. 7. This led to a non-interactive program which used a group of pores whose radii were in geometric progression with a common ratio F. As shown in the flow diagram given in Fig. 8, the program first of all determined the single pore radius R_0, which gave the best fit to the [$K(r)$, ln r] data and then determined β taking α as unity. Additional pores

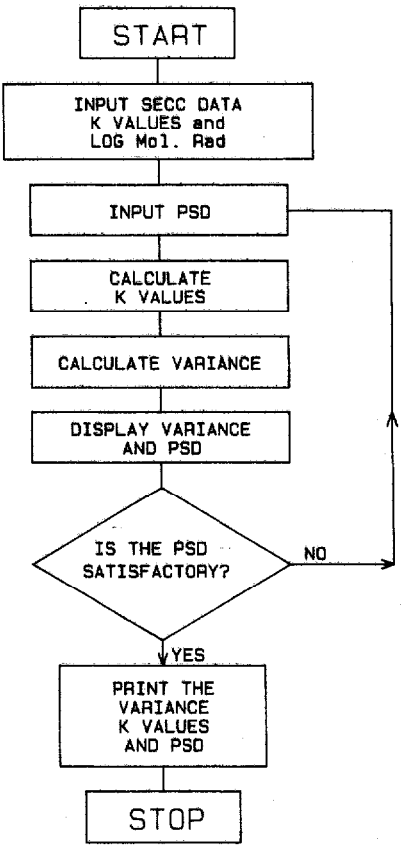

Fig. 7. Flow diagram for interactive computation of optimum PSD using a set of pores of assumed radii.

were then added successively in the order R_0F, R_0/F, R_0F^2, R_0/F^2, R_0F^3, R_0F^4.

This asymmetric distribution of pore sizes around the optimum single pore was used as experience showed that the low radius end of the [$K(r)$, ln r] curve was generally well fitted even by a single pore radius whereas the high radius end of the curve nearly always required additional pore sizes. It is at the high molecular weight end near the exclusion limit that the greatest flexibility is required.

Method 3B. Optimisation of α, β and volume fractions of a set of pores of preselected radii using EMAS

The use of the Edinburgh Multi-Access System (EMAS) mainframe computer at the Edinburgh Regional Computing Centre (ERCC, Edinburgh, U.K.) greatly accelerated the optimisation procedure and provided access to the highly sophisticated routines available from the ERCC library, in particular the program named MINUIT described in detail by James and Roos[17], which enabled up to 15 parameters to be optimised. Eqn. 11 for the variance V was expanded by incorporating eqns. 8 and 10 to give eqn. 15:

$$V = \sum_{\substack{\text{data}\\\text{points}}} \left\{ [\alpha + \beta K(r)_{\text{exp}}] - \sum_{\substack{R=r\\\text{pore}\\\text{sizes}}}^{R=\infty} F(R) \left(1 - \frac{r}{R}\right)^2 \right\}^2 \qquad (15)$$

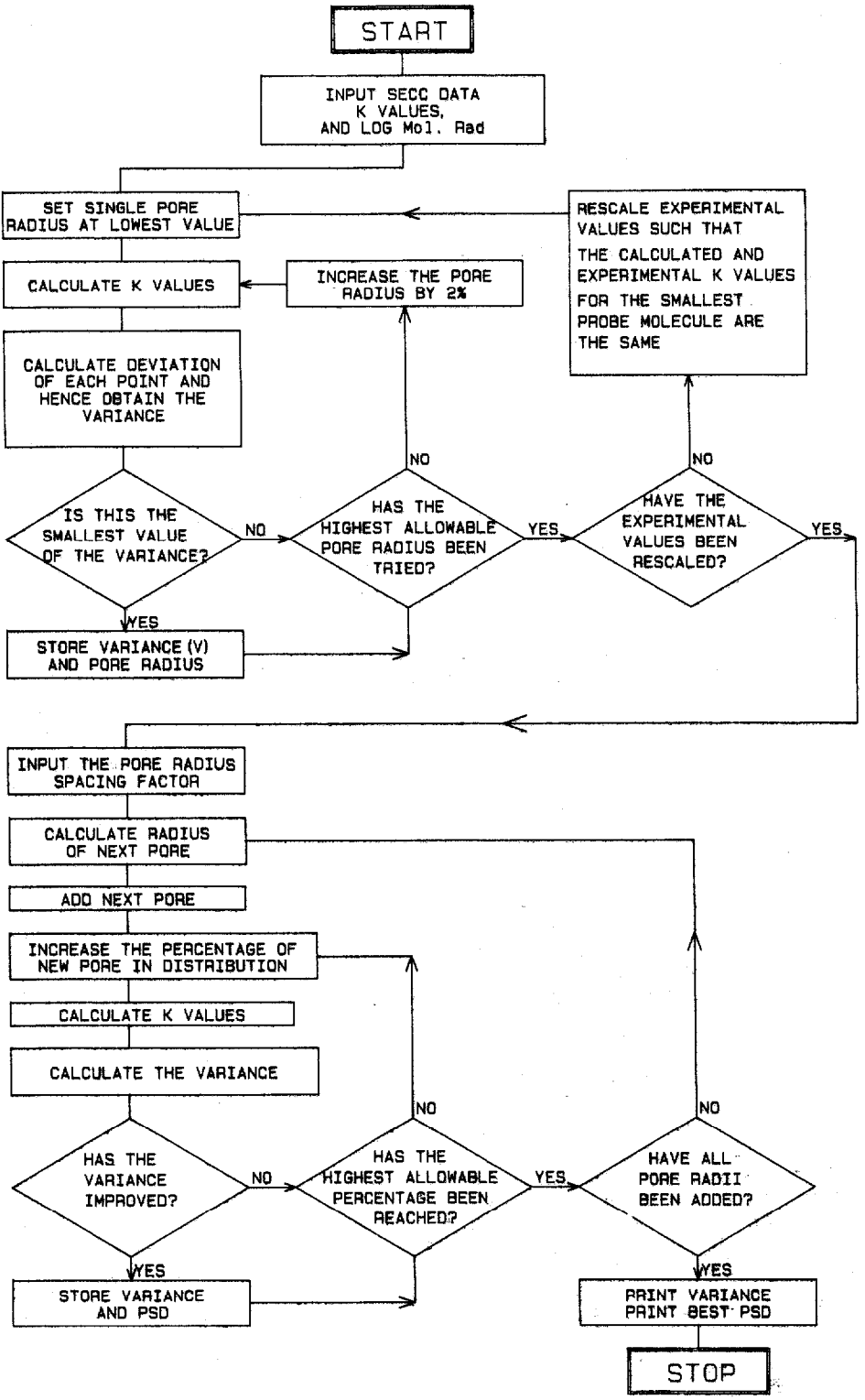

Fig. 8. Flow diagram for non-interactive computation of optimum PSD using a set of pores of assumed radii.

where the first term in the major summation is K_{adj} and the second term is K_{th}. Using eqn. 15 the values of α and β plus those of the $F(R)$ could all be optimized to give the lowest value of V. With seven discrete pore radii, as used in procedure 3A, only six are independent since

$$\sum_{i=1}^{7} F_i = 1 \tag{16}$$

Optimisation was therefore carried out for the eight parameters α, β, F_1, F_2, F_3, F_4, F_5, F_6, under the conditions that $(\alpha + \beta)$ and all seven F_i must lie between 0 and 1 and that neither α nor β can be negative. Initially the computer was provided with starting trial values of the eight parameters along with limits within which the final values should fall. MINUIT contains a number of optional subroutines of which we have used SIMPLX and MIGRAD.

SIMPLX is a simplex routine which minimises a function of N variables. In our case the function was V of eqn. 15 and N was eight. A simplex is a figure in N-dimensional space defined by a convex hull of $(N + 1)$ points (for example a triangle in two dimensions). Each point represents one possible set of the N parameters and corresponds to a single value of V. To construct the initial simplex S_0 from which the minimisation procedure starts, a particular set of the N parameters is chosen to define a starting point P_0. The remaining N points, P_1 to P_N, are then found by proceeding from P_0 in the directions of the N coordinate axes and determining the positions of minimum V in each of these directions.

At each performance of the subroutine a new simplex S_i is generated from simplex $S_{(i-1)}$. The routine first of all identifies P_W which has the highest value of V. The point P_W is then reflected in the $(N + 1)$ dimensional hyperplane through the remaining N points of the simplex to give P*, and V(P*) is then calculated.

Various alternatives are now open depending upon whether or not V is sufficiently reduced by the procedure. The procedures in ranking order are as follows:

(a) replace P_W by P*.

(b) IF V(P*) is not a sufficient improvement on $V(P_W)$ THEN find the point P** on the line P_WP* which gives minimum V; replace P_W by P**.

(c) IF V(P**) is not a sufficient improvement on $V(P_W)$ THEN find the point P*** on the parabola through P_WP*P** which has minimum V; replace P_W by P***.

(d) IF improvement is still inadequate THEN choose the point P_L giving the lowest V in the simplex and construct a new simplex with all dimensions reduced by a factor of 2.

(e) IF improvement still inadequate THEN construct a new simplex starting at P_L.

Following the above routine successive simplices produce a convergence of V towards a minimum and the algorithm terminates when the values of V at the P_W and P_B (the worst and best points in the simplex) coincide within the required accuracy.

The second minimisation subroutine named "MIGRAD" is a second order "steepest descents" algorithm. From a starting set of parameters giving a particular value of V, the routine calculates matrices of gradients and second derivatives of V

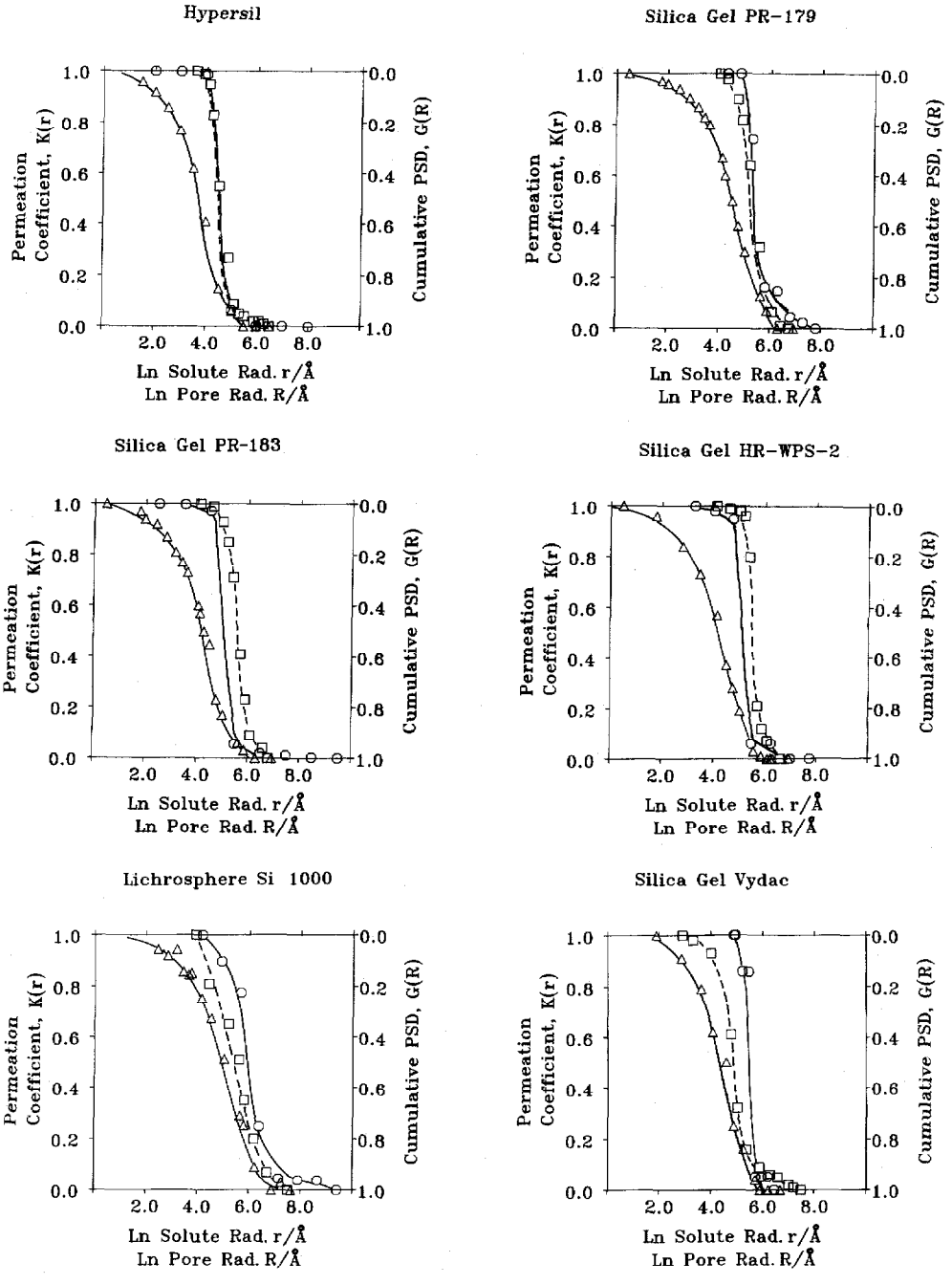

Fig. 9.

(*Continued on p. 80*)

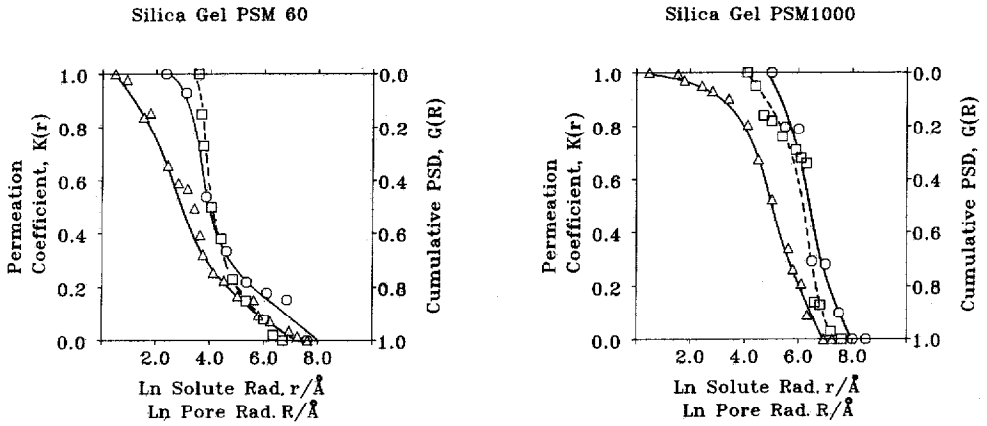

Fig. 9. Optimum PSDs derived from SECC data for eight silica gel samples using mainframe computer and MINUIT optimisation routine (method 3B). △, SECC data; □, PSD by Mercury porosimetry; ○, PSD by computation. Silica gels were: Hypersil (Shandon Southern Products); PR-179 and PR-183 (Experimental materials, Shandon Southern Products); HR-WPS-2 (Experimental material, this work); LiChrosphere Si 1000 (Merck); Vydac (Varian Assoc.); PSM60 and PSM1000 (DuPont SEC materials).

with respect to the N parameters. From this the direction of steepest descent and the estimated position of the minimum V are found. The procedure is then repeated starting at this new position in N-dimensional parameter space. MIGRAD tends to find local minima within a "minimum trough" and is most useful when performed after completion of the simplex routine as a form of fine tuning.

As a final check the "MIGRAD" routine moved a large distance from the position of the previously found optimum to check that no better solutions existed. In practice, SIMPLX provided satisfactory minima and MIGRAD used subsequently produced only marginal improvements.

The results obtained using these procedures are shown in Fig. 9 where the derived PSDs are compared to those found by mercury porosimetry for eight representative silica gels. Reasonable agreement is found in most cases.

Discussion

The major contribution made by Knox and Scott[13] to the derivation of PSDs from SECC data was to correct the error embodied in the method of Halasz and Martin[11,12]. The effect of this error is shown in Fig. 10 where three methods of deriving the PSD are compared. The Halasz method involves the simple displacement of the SECC curve to values of pore radii equal to 2.5 times the molecular radii. The PSD so obtained bears little relation to the PSD derived by mercury porosimetry or by computation according to method 3B except that it gives a reasonable value for the mean pore diameter [that is the pore diameter at $G(R) = 0.5$].

Fig. 11 shows that the non-interactive program using method 3A with a BBC microcomputer gives a good correlation between the PSD from mercury porosimetry and from computation, while Fig. 9 shows similar good agreement using method 3B with a mainframe computer for a range of commercial and experimental silica gels.

We have commented adversely on method 1 whereby a polynomial is fitted to

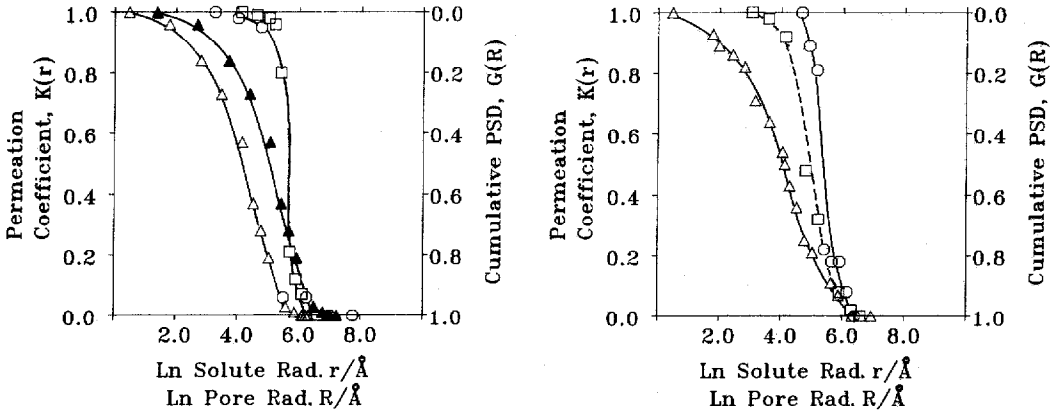

Fig. 10. Comparisons of PSDs derived by the Halasz method (▲), by method 3B of this work (○), by Mercury porosimetry (□). SECC data represented by △.

Fig. 11. Example of optimised PSD derived from SECC data for silica gel WP-10-04 (experimental wide pore material, Shandon Southern Products) using BBC Microcomputer (method 3A). △, SECC data; □, PSD by Mercury porosimetry; ○, PSD by computation.

the [$K(r)$, ln r] data and this subsequently differentiated to give the PSD. However, Fig. 12 shows that if the PSDs derived using a 6th degree polynomial fit to the [$K(r)$, ln r] data are simply truncated when $G(R)$ goes outside the range 0 to 1 the resulting curve is fairly close to that obtained by method 3. While this technique is not intellectually satisfying and has not been extensively studied by us it could nevertheless provide an acceptable method of obtaining a reasonable PSD fairly simply.

Table I compares the mean pore radius, $\bar{R}$, defined as the value of R for $G(R) = 0.5$ with the manufacturer's stated pore radius, and with the mean molecular radius, $\bar{r}$, defined as the value of r for which $K(r) = 0.5$. The ratio $\bar{R}/\bar{r}$ is the "Halasz Factor" giving the shift in the $K(r)$ curve required to give the best fit to the true PSD curve. This appears to be in the range 2.5 to 3.5 with a mean of about 3.0 rather than the value given by Halasz and Martin of 2.5.

Bearing in mind that the values of $\bar{R}$ and $\bar{r}$ are somewhat subjective, with uncertainties of around 10%, there is reasonable agreement for the majority of materials between the $\bar{R}$ values determined by mercury porosimetry and by unfolding the SECC curve. However both values are often at substantial variance with those quoted by the manufacturers even if there is broad agreement in so far as the supposed wide-pore materials do indeed have much wider pores according to our method than the supposed narrow-pore materials.

Use of the SECC unfolding technique clearly distinguishes between the different types of PSD exhibited by different materials. As can be seen from Figs. 9–11. The first five materials in Table I have a narrow PSD with 95% of the pores within a ten-fold range of diameter. LiChrosphere Si 1000 has a somewhat wider PSD with 95% of the pores within a roughly twenty-fold range, while the PSM materials have substantially wider PSDs with 95% of the pores within a fifty-fold range. Vydac and WP-10-04 are unusual in exhibiting a large difference between positions of the mercury porosimetry and SECC calculated PSD curves. This may indicate ink-bottle

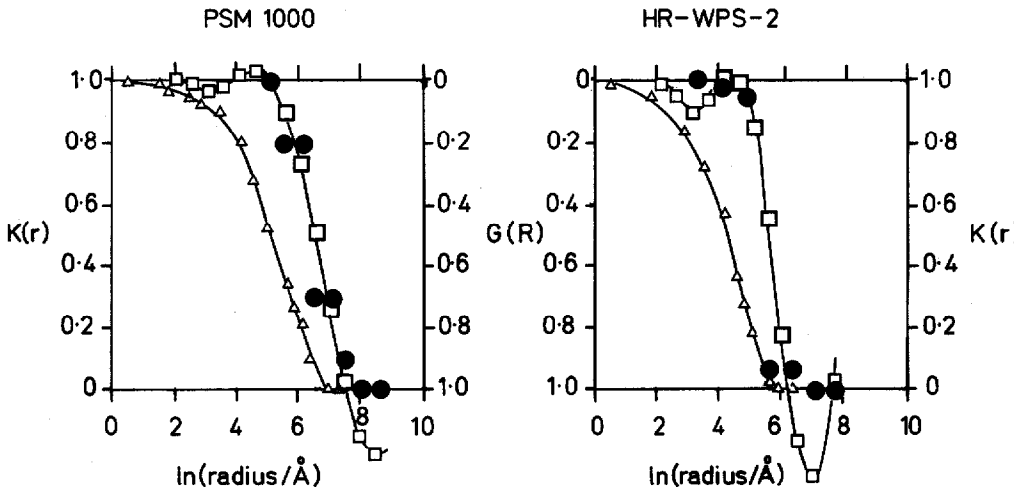

Fig. 12. Comparison of PSD derived by method 1 after truncation of fitted curve (see text) with that derived by method 3 for silica gel HR-WPS-2 (experimental batch this work) and PSM1000 (DuPont). △, SECC data [$K(r)$, ln r]; □, PSD by method 1; ●, PSD by method 3.

pores or that the particles have an outer surface layer with smaller pores than those inside the particles.

EXPERIMENTAL

Materials

Both commercial silica gels and batches of experimental materials were examined. Their physical properties along with the dimensions of the columns used for obtaining the SECC curves are listed in Table II.

TABLE I

MEAN PORE RADII FOR SEC MATERIALS

Material (Fig.)	*Mean solute radius* $\bar{r}$ *(Å)**	*Mean pore radius* $\bar{R}$ *(Å)*			*Halasz factor* $H = \bar{R}/\bar{r}$ *($\bar{R}$ is computed)*
		*By Hg porosimetry***	*By computation***	*Manufacturers value****	
Hypersil (9)	45	110	110	65	2.4
PR-179 (9)	95	230	270	–	2.9
PR-183 (9)	70	280	180	–	2.7
WP-10-04 (11)	65	130	220	150	3.3
HR-WSP-2 (9)	70	270	270	–	2.9
LiChrosphere Si 1000 (9)	165	300	470	500	2.8
Vydac (9)	80	140	280	–	3.5
PSM60 (9)	25	60	60	30	2.3
PSM1000 (9)	170	630	630	500	3.7
				Mean	2.94

* $\bar{r}$ is value of r at which $K(r) = 0.5$.

** $\bar{R}$ is value of R at which $G(R) = 0.5$.

*** Manufacturers' normally quote the pore diameter, these values are half the diameter.

Hypersil is a commercial silica gel manufactured by Shandon Southern Products. PR-179, PR-183 and WP-10-04 were experimental batches of wide-pore silica gels from the same supplier. HR-WPS-2 was an experimental wide pore material made for this work in the University of Edinburgh Chemistry Department. LiChrosphere Si 1000 is a commercial silica gel manufactured by Merck (Darmstadt, F.R.G.). Vydac is a commercial silica gel obtained from Varian Assoc. PSM60 and PSM1000 materials were obtained as packed columns from DuPont.

Equipment and chromatography

Surface areas were determined with nitrogen using a laboratory constructed BET equipment. Pore volumes and PSDs were determined by mercury intrusion porosimetry using a Micromeritics pore sizer, Model 9305. The data handling package calculated the pore size using eqn. 2 with a contact angle of 130°.

High-performance SEC was performed on home assembled equipment comprising an Altex 110A high-pressure pump, a Rheodyne 7125 injection valve and a Spectroflow 773 ultraviolet photometric detector (Kratos, Manchester, U.K.).

Details of the column and particle dimensions for each material are given in Table II. The Zorbax materials were supplied prepacked in DuPont columns. The remainder of the materials were packed into Shandon type columns using a Shandon packing system. Isopropanol was used as the dispersing liquid for the slurry and methylene chloride as the follower liquid. The packing was carried out at 200 bar. Solutes were polystyrene standards of polydispersity less than 1.1, obtained from Polymer Labs. (Church-Stretton, U.K.). All solvents were of HPLC-grade supplied by Rathburn Chemicals (Walkerburn, U.K.).

Computing equipment

The microcomputer was a BBC Model B made by Acorn Computers (Cambridge, U.K.). The more powerful optimization was carried out using a program named MINUIT devised by the Cern Computer Centre (Cern, Switzerland). This program was operated on the Edinburgh Multi-Access System (EMAS) at the Edinburgh Regional Computing Centre (ERCC).

TABLE II

PARTICLE PROPERTIES AND COLUMN DIMENSIONS

Material	*Particle size (μm)*	*Surface area ($m^2\ g^{-1}$)*	*Pore volume ($cm^3\ g^{-1}$)*	*Dimensions of test column (mm)*
Hypersil	5	176	0.68	250 × 4.6
PR-179	5	59	0.63	250 × 5.0
PR-183	5	74	0.64	250 × 5.0
WP-10-04	5	93	0.53	250 × 5.0
HR-WPS-2	5–10	90	1.30	100 × 4.6
LiChrosphere Si 1000	10	–	0.98	250 × 4.6
Vydac	5	71	0.46	250 × 5.0
Zorbax PSM60	5	–	0.47	250 × 6.2
Zorbax PSM1000	5	–	0.37	250 × 6.2

CONCLUSIONS

We have demonstrated that PSDs of silica gels used for HPLC may be derived by "unfolding" SECC data.

The best procedure optimises the volume fractions of a group of up to seven pores whose radii are in geometric progression. This can be achieved using a microcomputer, or more efficiently using a mainframe computer.

Computed PSDs agree well with those found by mercury porosimetry.

The method of Halasz and Martin[11,12] gives a reasonable value for the mean pore size of a material but too small a slope for the PSD curve, especially for materials with a narrow PSD. The "Halasz Factor" should however be taken as 3.0 rather than 2.5.

We recommend that the methods developed in this paper be employed to determine PSDs of mesoporous materials especially when they are to be employed for size exclusion and other forms of liquid chromatography.

ACKNOWLEDGEMENTS

The authors thank Mr. Paul Ross from Shandon Southern Products Ltd. for carrying out the mercury porosimetry measurements, Mr. Gavin Gibson and Mr. Alastair Brown for their help with the computing throughout the project and Dr. Neil R. Herbert of Shandon Southern Products Ltd. for encouragement and advice in his capacity as industrial supervisor of the work carried out under the Cooperative Award in Science and Engineering Scheme of the Science and Engineering Research Council.

REFERENCES

1 K. K. Unger, *Porous Silica (Journal of Chromatography Library*, Vol. 16), Elsevier, Amsterdam, 1979.
2 S. Brunauer, P. H. Emmett and E. Teller, *J. Am. Chem. Soc.*, 60 (1938) 309.
3 S. J. Gregg and K. S. W. Sing, *Adsorption, Surface Area and Porosity*, Academic Press, London, 1967.
4 R. Beau, M. Le Page and A. J. De Vries, *Appl. Polym. Symp.*, 8 (1969) 137–155.
5 E. F. Casassa, *J. Phys. Chem.*, 75 (1971) 3929.
6 I. Halasz and W. Werner, *Chromatographia*, 13 (1980) 271.
7 F. Nevejans and M. Verzele, *Chromatographia*, 20 (1985) 173.
8 I. Halasz, W. Werner and R. Nikolov, *J. Chromatogr. Sci.*, 18 (1980) 207.
9 T. Crispin and I. Halász, *J. Chromatogr.*, 239 (1982) 351.
10 R. Groh and I. Halasz, *Anal. Chem.*, 53 (1982) 1325.
11 I. Halasz and K. Martin, *Ber. Bunsenges. Phys. Chem.*, 79 (1975) 731–734.
12 I. Halasz and K. Martin, *Angew. Chem. Int. Ed. Engl.*, 17 (1978) 901–908.
13 J. H. Knox and H. P. Scott, *J. Chromatogr.*, 316 (1984) 311–332.
14 G. V. Schulz and H. Baumann, *Makromol. Chem.*, 114 (1968) 122.
15 M. E. van Kreveld and N. van den Hoed, *J. Chromatogr.*, 83 (1973) 111–124.
16 F. V. Warren and B. R. Bidlingmeyer, *Anal. Chem.*, 56 (1984) 950–957.
17 F. James and M. Roos, *Comput. Phys. Commun.*, 10 (1975) 343–367.